Electrically driven nanoarrow array green LED

J.-R. Chang[a], S.-P. Chang[b], Y.-C. Chen[b], K.-P. Sou[b], Y.-J..Cheng[b, c]*, H.-C. Kuo[b], and C.-Y. Chang[a]

[a] Dept. of Electronic Engineering, National Chiao Tung University, 1001 Ta Hsueh Rd., Hsinchu 300, Taiwan;

[b] Dept. of Photonics, National Chiao Tung University, 1001 Ta Hsueh Rd., Hsinchu 300, Taiwa;

[c] Research Center for Applied Sciences, Academia Sinica, Taipei 11529, Taiwan.

ABSTRACT

An electrically driven nanopyramid green light emitting diode (LED) was demonstrated. The nanopyramid arrays were fabricated from a GaN substrate by patterned nanopillar etch, pillar side wall passivation, and epitaxial regrowth. Multiple quantum wells were selectively grown on the facets of the nanopyramids. The fabricated LED emits green wavelength under electrical injection. The emission exhibits a less carrier density dependent wavelength shift and higher internal quantum efficiency as compared with a reference c-plane sample at the same wavelength. It shows a promising potential for using nanopyramid in high In content LED applications.

Keywords: semipolar, GaN, LEDs.

1. INTRODUCTION

Light emitting semiconductor devices in green color has attracted great interest in lighting and display applications [1-3]. Conventionally, GaN based light emitting diodes are often fabricated on c-plane GaN surface. The emission wavelength is typically in the blue region, where its performance is optimal. Multiple quantum wells (MQWs) grown on this crystal plane experience an internal electric field (IEF) due to spontaneous and piezoelectric polarization, which can significantly reduce internal quantum efficiency (IQE) [4,5]. The efficiency drops rapidly as In content increases in MQWs for green emission due to the increased IEF [6]. This IEF can also cause carrier density dependent wavelength shift. To overcome these detrimental effects, an attractive approach is to grow MQWs on nonpolar or semipolar crystal planes, which have no or lower IEF and can accommodate high In incorporation [7]. Green LEDs and lasers fabricated on semipolar GaN substrates have gained significant interests recently [8-12]. However, nonpolar and semipolar substrates are not readily available. Selective area growth is an attractive alternative method to grow semipolar facets from the widely available c-plane substrates. Micro to nano size hexagonal pyramids can be grown from the opening holes of a SiO_x or SiN_x masked c-plane GaN substrate. The pyramid facets are typically {10-11} or {11-22} semipolar planes. The Photoluminescent (PL) study of the MQWs grown on semipolar pyramid facets has shown significantly reduced the carrier density dependent wavelength shift and inhomogeneous In distribution [13][14]. There have been interests in using the semipolar pyramid facets for green InGaN LED applications [[13]-[16]], but so far the reports are mostly limited to optical pumping. Reports on electrical injection are very limited [[16]]. Here, we report the fabrication and performance of an electrically driven nanopyramid green LED. Compared with a reference c-plane MQW LED, the PL measurement have shown less carrier density dependent blue shift and significantly enhanced IQE.

2. EXPERIMENT

The device was fabricated from an n-type GaN substrate grown on a c-plane sapphire template by AXITRON 2000HT metal organic chemical vapor deposition (MOCVD) reactor. The scanning electron microscopy (SEM) images of the intermediate fabrication steps are shown in Fig. 1(a)-(d). SiO_2 nano disks of 250 μm in diameter were first patterned on a GaN substrate. The SiO_2 disks were used as etching masks in inductively coupled plasma reactive ion etching (RIE). The

* yuhjen_cheng@yahoo.com; phone 886 3 5752726

Light-Emitting Diodes: Materials, Devices, and Applications for Solid State Lighting XVI,
edited by Klaus P. Streubel, Heonsu Jeon, Li-Wei Tu, Norbert Linder, Proc. of SPIE Vol. 8278,
827815 · © 2012 SPIE · CCC code: 0277-786X/12/$18 · doi: 10.1117/12.907749

Downloaded From: http://proceedings.spiedigitallibrary.org/ on 04/28/2014 Terms of Use: http://spiedl.org/terms

SiO_2 disks were subsequently removed by a buffer oxide etch, leaving arrays of GaN nanopillars (Fig. 1(a)). Spin-on glass was spun on the substrate to planerize the surface. After curing the spin-on glass at 400 ^oC for 60 min., the nanopillar side walls were covered by spin-on glass with air voids among them. The air voids were created due to the shrinkage of spin-on glass during curing process. The substrate was then etched by RIE to expose the top portion ofnanopillars while leaving nanopillar side walls still covered with spin-on glass (Fig. 1(b)). The substrate was put back into MOCVD for GaN epitaxial regrowth. GaN pyramids were selectively grown on the tops of nanopillars at growth pressure of 600 mbar and temperature of 800 ^oC with growth rate of about 0.5 μm/hr (Fig. 1(c)). The pyramid facets were identified as semipolar {10-11} plane from its inclined 62° angle. Ten pairs of $In_{0.3}Ga_{0.7}N$(~2 nm)/GaN(~8nm) MQWs were grown on the pyramid facets, followed by a 20-nm electron blocking layer of Mg-doped p-type $Al_{0.15}Ga_{0.85}N$ and a 200-nm Mg-doped p-type GaN layer. The growth temperature of GaN and InGaN were 800 ^oC and 710 ^oC, respectively. The MQW growth pressure was 300 mbar. The TMIn and TMGa flux were 250 and 76 sccm. Figure 1(d) shows the plane view of the fabricated LED. The surface was rough due to the nanopyramid structure. For comparison, a conventional c-plane MQW substrate was grown on a c-plane sapphire template. The MQW growth parameters were similar except that the barrier and well growth temperature were raised to 820 ^oC and 730 ^oC, respectively, to obtain similar emission wavelength.

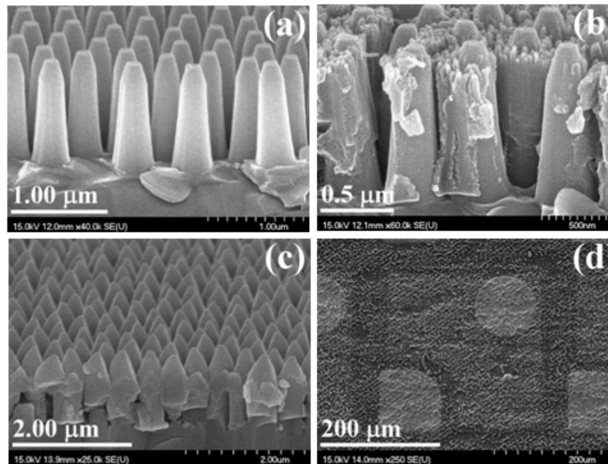

Figure 1(a)-(d). SEM images of intermidiate fabrication steps. (a) Etched nanopillar. (b) Side wall coated with spin-on glass. (c) Nanopyramids grown on nanopillars (d) Plane view of nanopyramid LED.

3. RESULT AND DISCUSSION

The emission properties of the fabricated {10-11} and {0001} MQW samples were investigated by photoluminescent (PL) measurement. The samples were optically excited by a Ti:sapphire pulse laser at wavelength of 400 nm focused down to a spot diameter of approximately 50 um on the sample. The repetition rate was 76 MHz, and the pulse width was 0.2 ns. The measured PL peak wavelength versus excitation power density is shown in Fig. 2(a). The {0001} MQW sample had a blueshift of 45 nm when the pump intensity was increased from 1 W/cm^2 to 2.5 kW/cm^2. In contrast, the {10-11} MQW sample had a blueshift of only 10 nm within the same pump intensity range. The blueshift was due to the screening of IEF by the excited carriers and the filling of localized potential fluctuations induced by inhomogeneous In distribution in MQWs. The observed smaller blueshift of {10-11} MQWs is consistent with previous reports. The carrier life time was measured by a time resolved PL (TRPL) system (PicoHarp 300) at low temperature (LT) 15K and room temperature (RT). The measured TRPL signals are shown in Fig. 2(b). The fitted decay time of {10-11} ({0001}) MQWs at LT and RT were 0.21 (85) and 0.11 (8) ns, respectively. The recorded linear decrease of PL intensity of {0001} MQWs at LT was due to the short recording period limited by the pulse laser repetition rate. We assumed that it was an exponential decay and extracted the life time constant by the approximation $\exp(-t/\tau) \sim 1- t/\tau$, when $t << \tau$. The obtained 85 ns time constant is much larger than the recording period of 13 ns. The approximation is thus justified. The sub-ns life time of {10-11} MQWs and high tens of ns life time of {0001} MQWs at LT have also been reported [[17]]. Non-

Downloaded From: http://proceedings.spiedigitallibrary.org/ on 04/28/2014 Terms of Use: http://spiedl.org/terms

radiative recombination is normally inactive at low enough temperature. The measured LT life time is therefore assumed to be due to radiative recombination. The shorter life time of {10-11} MQWs is again attributed to its lower IEF, which results in higher radiative recombination probability. At RT, the non-radiative recombination is normally not negligible, which causes the PL life time to become smaller and degrades the IQE.

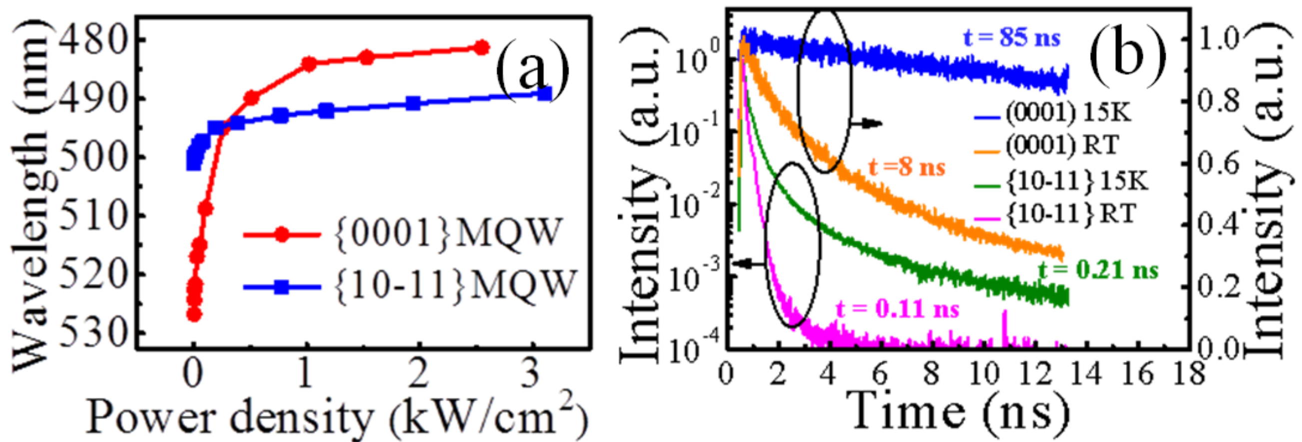

Figure 2. (a) PL peak wavelength versus pump power density of {10-11} and {0001} MQWs. (b) TRPL decay curves of {10-11} and {0001} MQWs at 15K and RT.

We measured the IQEs of these two samples. The IQE was obtained by normalizing the integrated PL intensity at room temperature by the value at 15K. The measurement was done at the pump power level where the efficiency was at maximum. The measured IQE of {10-11} and {0001} MQWs were 50% and 28%, respectively. It is worth to note that the IQE of {10-11} sample is enhanced by 79%, which is in large disparity to the two order of magnitude decrease in radiative lifetime, as compared with the {0001} sample. This discrepancy implies that the non-radiative recombination rate is also much faster for {10-11} sample. The radiative and non-radiative life time, τ_r and τ_{nr}, can be deduced from the measured PL life time τ_{PL} and IQE, which are related to τ_r and τ_{nr} by

$$\frac{1}{\tau_{PL}} = \frac{1}{\tau_r} + \frac{1}{\tau_{nr}} \tag{1}$$

and

$$IQE = \frac{1}{1 + \tau_r / \tau_{nr}} \tag{2}$$

From the measurement, the RT life time (τ_r, τ_{nr}) of {10-11} and {0001} MQWs are (0.22, 0.22) ns and (29, 11) ns, respectively. The much shorter τ_{nr} of {10-11} sample could be attributed to the less localized potential fluctuations, as compared with {0001} sample. Previous experimental results suggest that the localized potential due to inhomogeneous In distribution may suppress the capture of carriers by non-radiative centers. The reduced localized potential fluctuations of {10-11} MWQ therefore increase the carrier capture probability by non-radiative centers and gives shorter τ_{nr}.

The spatial dependent emission property of nanopyramids was investigated by the spectrally resolved cathodoluminescent (CL) measurement. A plane view scanning electron microscope (SEM) image was first taken, as shown in Fig. 3(a). The spectrally resolved CL images were then scanned at 500, 540, and 560 nm, as shown in Fig. 3(b)-(d). The emission pattern basically follows the pyramid height contour, as can be seen by comparing the bright

Downloaded From: http://proceedings.spiedigitallibrary.org/ on 04/28/2014 Terms of Use: http://spiedl.org/terms

contours in Fig. 3(b)-(d) to the pyramid shape in SEM image Fig. 3(a). The contours move toward the tips of nanopyramids as wavelength increases. It indicates that the MQW emission redshifts from the bottom to top region of nanopyramids. This may be due to the increase of In incorporation and IEF in MQWs as the region moves up the nanopyramid facet.

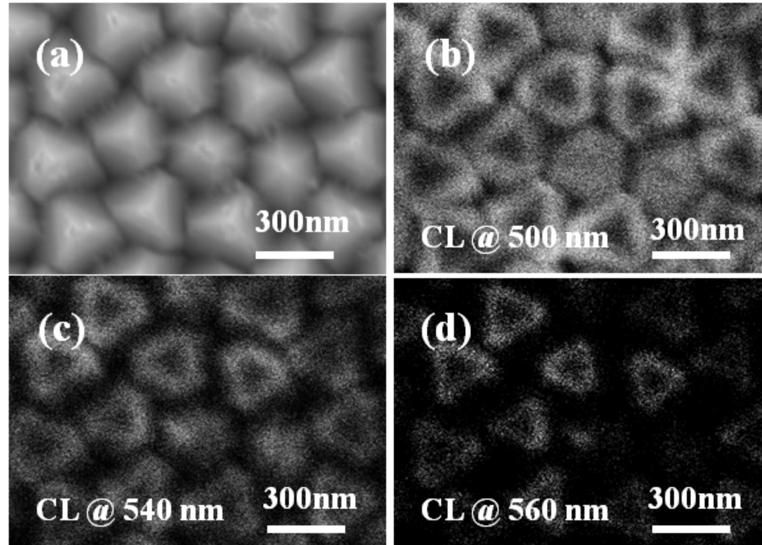

Figure 3. (a) SEM plane view of nanopyramid LED. (b)-(d) Spectrally resolved CL images at 500, 540, and 560 nm.

The {10-11} MQW substrate was fabricated into a 300 μm x 300 μm LED chip using standard LED fabrication steps. The microscope image of the electrically driven LED exhibits a bluish green emission as shown in Fig. 4(a). The dark regions are the p- and n-metal contacts. The light-current-voltage (L-I-V) curves of the fabricated nanopyramid LED chip are shown in Fig. 4(b). The L-I curve shows a slow turn on of light. When the current is at 5 mA, the steep increase of voltage starts to level off at 2.3 volt while light output is still negligible. This could be due to some growth defects and process imperfection that provide shunt paths to the current. The coalescent boundaries among nanopyramids could be one of the possible causes. After turn on, the driving voltage increases substantially from 3 volt to 7 volt as current increases up to 200 mA. This high voltage is probably due to a high contact resistance between ITO and the non-planar surface of nanopyramid arrays. Process optimization is required for a further improvement. The EL spectrum versus injection current is shown in Fig. 4(c). At low injection current, emission peak starts at 625nm and blueshifts as current increases (inset of Fig. 4(c)). The emission peak is stabilized around 495 nm above 50 mA, as depicted by the dotted line. The spectrum has a broad linewidth of ~57 nm and a long tail extended beyond 600 nm. There are small Fabry-Perot oscillation ripples with ~8.25 nm spacing. It corresponds to a cavity length of ~6 μm, which is close to the total GaN thickness. The ripple is probably due to the reflection between pyramid facets, acting like corner cube, and the sapphire/GaN interface. From the CL measurement, the initial long wavelength emission is likely from the apex region of MQWs, which is turned on first because the potential is lower. As the current increases, the injected carriers overflow to the lower portion of MQWs. The emission thus shifts to 495 nm and becomes the dominant peak because of the much larger MQW area.

Downloaded From: http://proceedings.spiedigitallibrary.org/ on 04/28/2014 Terms of Use: http://spiedl.org/terms

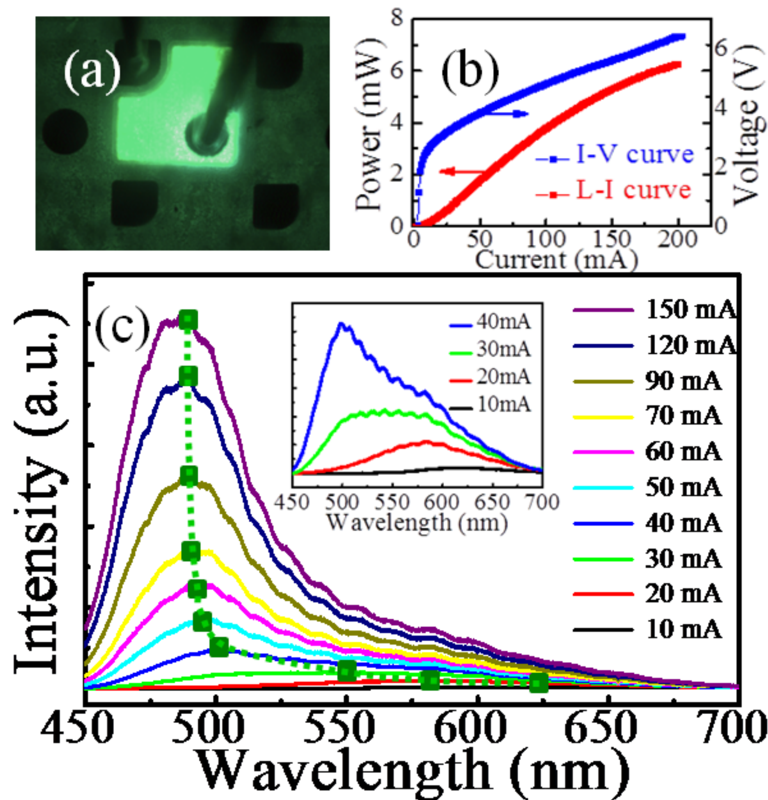

Figure 4. (a) Microscope image of electrically driven nanopyramid green LED. (b) L-I-V curves of nanopyramid LED. (c) PL spectrum versus injection current. Inset is the low current PL spectra.

4. CONCLUSION

In summary, we have demonstrated an electrically driven nanopyramid LED. The nano-arrow arrays were fabricated from a GaN substrate, by patterned top-down nanopillar etching, pillar side wall passivation, and epitaxial regrowth. Hexagonal pyramids were formed on top of nanopillars. Quatnum wells (QWs) were grown on the pyramid semipolar planes, which allows higher In incorporation. The fabricated LED emits at 500 nm. The LED shows enhanced radiative recombination efficiency and less carrier density dependent wavelength shift compared with a LED grown on c-plane surface. The performance improvement is attributed to the reduced polarization field in QWs grown on semipolar plane. This demonstration shows a promising potential for developing high In composition LEDs by using semipolar MQWs grown on nanopyramids, which can be fabricated from readily available c-plane sapphire substrates.

REFERENCES

[1] K. S. Kim, J. K. Son, S. N. Lee, Y. J. Sung, H. S. Paek, H. K. Kim, M. Y. Kim, K. H. Ha, H. Y. Ryu, O. H. Nam, T. Jang, and Y. J. Park, Appl. Phys. Lett. 92, 101103 (2008)

[2] D. Queren, A. Avramescu, G. Brüderl, A. Breidenassel, M. Schillgalies, S. Lutgen, and U. Strauß, Appl. Phys. Lett. 94, 081119 (2009).

[3] T. Miyoshi, S. Masui, T. Okada, T. Yanamoto, T. Kozaki, S.-I. Nagahama, and T. Mukai, Appl. Phys. Express 2, 062201 (2009).

[4] Y. L. Lai, C. P. Liu, Y. H. Lin, R. M. Lin, D. Y. Lyu, Z. X. Peng, and T. Y. Lin, Appl. Phys. Lett. 89, 151906 (2006).

Downloaded From: http://proceedings.spiedigitallibrary.org/ on 04/28/2014 Terms of Use: http://spiedl.org/terms

[5] F. Bernardini, V. Fiorentini, and D. Vanderbilt, Phys. Rev. B 56, R10024 (1997).
[6] D. Fuhrmann, C. Netzel, U. Rossow, A. Hangleiter, G. Ade, and P. Hinze, Appl. Phys. Lett. 88, 071105 (2006).
[7] H. Sato, R. B. Chung, H. Hirasawa, N. Fellows, H. Masui, F. Wu, M. Saito, K. Fujito, J. S. Speck, S. P. DenBaars, and S. Nakamura, Appl. Phys. Lett. 92, 221110 (2008).
[8] H. Zhong, A. Tyagi, N. N. Fellows, F. Wu, R. B. Chung, M. Saito, K. Fujito, J. S. Speck, S. P. DenBaars, and S. Nakamura, Appl. Phys. Lett. 90, 233504 (2007).
[9] K. Okamoto, J. Kashiwagi, T. Tanaka, and M. Kubota: Appl. Phys. Lett. 94 071105 (2009).
[10] A. Tyagi, Y. D. Lin, D. A. Cohen, M. Saito, K. Fujito, J. S. Speck, S. P. DenBaars, and S. Nakamura, Appl. Phys. Express 1, 091103 (2008).
[11] H. Asamizu, M. Saito, K. Fujito, J. S. Speck, S. P. DenBaars, and S. Nakamura, Appl. Phys. Express 1, 091102 (2008).
[12] Y. Enya , Y. Yoshizumi, T. Kyono, K. Akita, M. Ueno, M. Adachi, T. Sumitomo, S. Tokuyama, T. Ikegami, K. Katayama, and T. Nakamura, Appl. Phys. Express 2 082101 (2009).
[13] T. Kim, J. Kim, M.-S. Yang, S. Lee, Y. Park, U-I. Chung, and Y. Cho, Appl. Phys. Lett. 97, 241111 (2010).
[14] H. Yu, L. K. Lee, T. Jung, and P. C. Ku, Appl. Phys. Lett. 90, 141906 (2007).
[15] C. Liu, A. Satka, L. K. Jagadamma, P. R. Edwards, D. Allsopp, R. W. Martin, P. Shields, J. Kovac, F. Uherek, and W. Wang, Appl. Phys. Express 2, 121002 (2009).
[16] I. H. Wildeson, R. Colby, D. A. Ewoldt, Z. Liang, D. N. Zakharov, N. J. Zaluzec, R. E. García, E. A. Stach, and T. D. Sands, J. Appl. Phys. 108, 044303 (2010).
[17] M. Funatoa and Y. Kawakami, J. Appl. Phys. 103, 093501 (2008).
[18] S. Watanabe, N. Yamada, M. Nagashima, Y. Ueki, C. Sasaki, Y. Yamada, T. Taguchi, K. Tadatomo, H. Okagawa, and H. Kudo, Appl. Phys. Lett., 83, 4906, (2003).
[19] A. Sasaki, S. I. Shibakawa, Y. Kawakami, K. Nishizuka, Y. Narukawa, and T, Mukai, Jpn. J. Appl. Phys. 45, 8719 (2006).

Downloaded From: http://proceedings.spiedigitallibrary.org/ on 04/28/2014 Terms of Use: http://spiedl.org/terms